



LSMA 结合 NDBI 提取广州市部分城区不透水面的方法

赵怡^{1,2,3}, 许剑辉², 钟凯文², 王云鹏¹, 郑秋霞^{1,3}

(1. 中国科学院广州地球化学研究所, 广东广州 510640; 2. 广州地理研究所, 广东广州 510070; 3. 中国科学院大学, 北京 100049)

摘要:以广州部分城区为研究区, 选取 2015 年 10 月 18 日 Landsat 8 OLI 遥感影像, 基于线性光谱混合分析 (LSMA), 结合归一化建筑指数 (NDBI) 优化不透水面盖度提取精度; 并分别采用传统 LSMA 和优化 LSMA 提取了不透水面。在传统方法的基础上, 优化 LSMA 利用纯净像元指数与手动端元相结合的方法提高了端元选取精度; 解混后再利用 NDBI 阈值掩膜。经验证, 传统 LSMA 提取不透水面盖度的均方根误差 (RMSE) 为 0.306, 与样本区的相关系数 (R^2) 为 0.898, 系统误差 (SE) 为 0.21; 优化 LSMA 的 RMSE 为 0.125, 与样本区的 R^2 为 0.943, SE 为 -0.035, 精度明显高于传统 LSMA 的提取精度, 可为广州市不透水面环境效应研究提供更可信的数据支持。

关键词: LSMA; 手动选取; NDBI; 不透水面

中图分类号: P237

文献标志码: B

文章编号: 1672-4623 (2018) 03-0090-04

近年来城市快速发展, 森林、湿地和其他形式的开放空间减少^[1], 不透水面大量增加对环境有直接影响^[2], 如城市地表的扩增导致了城市热岛效应^[3-4], 同时使得地表径流发生变化, 成为城市内涝、暴雨天气的重要原因之一。因此, 高精度的不透水面提取对城市生态环境、水文气候的研究具有非常重要的意义。1995 年 Ridd 提出了植被—不透水表面—土壤 (V-I-S) 模型。V-I-S 模型将城市环境中土地覆盖假设为植被、不透水表面和土壤 3 个部分的线性组合^[5-6]。WU C S^[7]等基于 V-I-S 模型将城市地表类型分为 4 类端元, 并提出了线性光谱混合分析 (LSMA), 已成为广泛应用于中分辨率遥感影像中的不透水面反演方法^[8-17]。

遥感影像中不透水面基本表现为高反照率地表与低反照率地表的组合^[18], 不透水面盖度 (ISC) 是指某区域内不透水面覆盖面积与区域面积的比例^[19]。LSMA 可在亚像元尺度上提取 ISC, 端元选取是关键步骤^[20]。因混合像元 (如砂石和砂土等地物) 与不透水面光谱差异较小, 将影响端元精度, 导致透水表面区域 ISC 较高。樊风雷^[21]等利用相关指数掩膜低反照率不透水面的方法提高了提取精度, 但高反照率不透水面中的混合像元问题未曾涉及。本文在传统 LSMA 方法的基础上进行优化, 将纯净像元指数 (PPI) 与手动端元选取相结合, 以提高端元选取精度; 再利用 NDBI 阈值同时掩膜高低反照率不透水面盖度结果, 以提高 ISC 提取精度。

1 研究方法

本文以 2015 年 10 月 18 日广州市部分城区的 Landsat 8 OLI 遥感影像为研究对象, 经预处理, 运用改进归一化水体指数 (MNDWI)^[22] 去除水体; 分别采用传统 LSMA 和优化 LSMA 提取研究区的 ISC, 并选择同时相的 Google Earth 影像作为验证数据进行端元验证和 ISC 提取精度验证。

1.1 传统 LSMA

传统 LSMA, 假设影像中每个像元的反射率是该像元中所有地物端元的反射率以其所占像元面积比例为权重系数的线性组合^[23], 其数学模型为^[24]:

$$R_i = \sum_{k=1}^n f_k R_{ik} + ER_i \quad (1)$$

式中, $i=1, 2, \dots, M$, M 为光谱波段数; n 为端元数目; R_i 为波段 i 的反射率; f_k 为端元 k 在像元中所占面积比例; R_{ik} 为波段 i 上端元 k 的光谱反射率; ER_i 为波段 i 的残差。

通过每个波段的残差均方根 (RMS) 来检验解混模型的正确性:

$$RMS = \sqrt{\frac{\sum_{i=1}^M ER_i^2}{M}} \quad (2)$$

此外, 一个像元内所有端元的面积比例和为 1, 线性光谱模型在求解 f_k 时必须满足:

$$\sum_{k=1}^n f_k = 1 \text{ 且 } f_k \geq 0 \quad (3)$$

1.2 优化 LSMA

结合实际情况, 本文采用 PPI 结合手动端元选取

收稿日期: 2016-12-22。

项目来源: 广东省水利科技创新资助项目 (2015-13); 广东省自然科学基金资助项目 (2014A030313747); 广东省科学院实施创新驱动发展能力建设专项资金资助项目 (2017GDASCX-0804); 广东省科学院平台环境与能力建设专项资金资助项目 (2016GDASPT-0103)。

的方法以及归一化建筑指数 (NDBI) 阈值法提高 ISC 精度, 优化 LSMA 流程^[25-26] 如图 1 所示。

1.2.1 PPI 结合手动端元选取

传统 LSMA 是在 N 维空间中直接以像元纯净度为依据选取顶点离散的点, 一般以 10 作为纯净像元阈值选取 4 类端元: 植被、裸土、高反照率不透水面和低反照率不透水面。PPI 是常用的纯净像元提取方法, PPI 越高, 纯净度越高。PPI 高的端点一般位于 MNF 变换后散点图三角形的顶点位置。经过 PPI 阈值筛选后, 像元的数目大量减少, 但由于地表类型复杂, 仍然存在错分现象, 即选取的端元与目标类别不匹配。

手动端元选取的关键是通过目视、比较分析的方法选取地物类别典型地区, 获得较纯净的像元^[27]。根据 LSMA 原理, 只要满足端元数大于等于遥感影像的波段数, 线性方程组就可有解。本文中 PPI 高于 10 的像元极少且集中在森林区域。经比较, PPI 阈值设为 5, 再利用二维散点图, 手动继续选取影像空间顶点区域零散的点。将 4 类地物端元分别加载到经过配准的 Google Earth 高分辨率影像上, 继续去除错分端元。

1.2.2 NDBI 阈值法

传统 LSMA 解混结果中, 在部分土壤和大面积森林等透水面内, ISC 仍存在且比例较高。在 OLI 前 4 个波段高低反照率不透水面均与植被、土壤等透水面光谱有交集, 导致解混过程中产生错分现象; 而在波段 5、

波段 6 之间的光谱差异明显增大。针对这种情况, 本文利用 NDBI^[28] 对 ISC 提取结果进行掩膜处理。

$$NDBI = \frac{MIR - NIR}{MIR + NIR} \quad (4)$$

式中, MIR 为遥感影像的中红外波段; NIR 为遥感影像的近红外波段。

经统计发现, 计算的 NDBI 在 $-0.66 \sim 0.45$ 之间; 而通过与高分辨率影像的对比发现, 绝大部分不透水面的 NDBI 在 $-0.15 \sim 0.45$ 之间。理论上大于 0 的部分可被分为建筑; 而线性光谱解混是基于亚像元尺度的, 为了在像元尺度上尽可能地保证不透水面的基本范围, 选择 -0.15 、 -0.1 、 -0.05 和 0 分别对高低反照率 ISC 结果进行掩膜, 再通过高分辨率影像样本区进行验证, 最终确定阈值为 -0.15 。

1.3 精度验证

结合空间分辨率为 2 m 的 Google Earth 高分辨率影像, 经过几何校正, 确保校正误差小于 0.5 个像元。本文选取 100 个随机样本区域进行矢量化, 并实地验证, 统计实验结果中样本区的 ISC。OLI 影像空间分辨率为 30 m, 每个样本区域边长设置为 480 m。本文采用均方根误差 (RMSE)、系统误差 (SE)、平均绝对误差 (MAE) 以及相关系数 (R^2) 对 ISC 提取精度进行验证:

$$RMSE = \sqrt{\frac{\sum_{i=1}^N (\bar{X}_i - X_i)^2}{N}} \quad (5)$$

$$SE = \frac{\sum_{i=1}^N (\bar{X}_i - X_i)}{N} \quad (6)$$

$$MAE = \frac{\sum_{i=1}^N |\bar{X}_i - X_i|}{N} \quad (7)$$

式中, \bar{X}_i 为本文中从 Landsat 8 OLI 数据中提取的样本区域内不透水面的比例; X_i 为高分辨率验证影像样本区域内不透水面的比例; N 为样本数。

2 实验结果与分析

2.1 不透水面提取结果

利用 MNF 变换后的主成分生成散点图, 通常认为纯度高的端元靠近边缘。PPI 阈值为 10 时选取的端元光谱曲线如图 2 所示。土壤和高反照率端元光谱形状相似, 但高反照率端元的反射率相对较高。在前 4 个波段, 高反照率端元的反射率比植被端元的反射率高很多, 但在波段 5 植被端元的反射率反而比高反照率端元的反射率还高, 这将导致植被像元可能被误判为高反照率不透水面, 而本身属于高反照率不透水面的像元却未能被较好地识别。计算 PPI 后, 将 PPI 阈值调为 5, 掩膜 MNF 结果, 结合手动选取端元, 4 类端元光谱曲线如图 3 所示, 高反照率端元与植被明显分离。

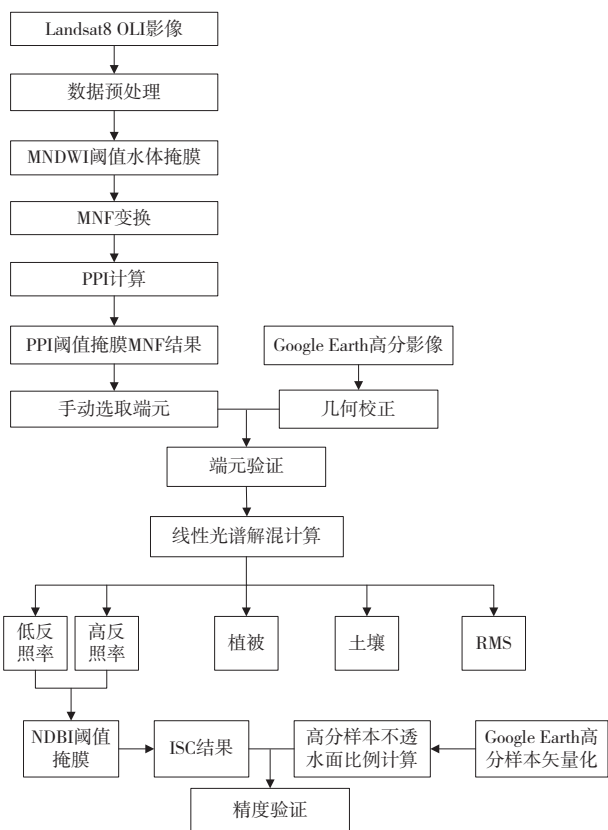


图 1 优化 LSMA 流程图

两种端元选取方式的解混结果如图 4a、4b 所示。经验证，后者城区 ISC 结果明显提高，如图 5a 所示，土壤和森林的 ISC 降低。图 4c 在图 4b 的基础上进行了 NDBI (-0.15) 阈值掩膜，经验证，去除了异常区域的不透水面，精度大幅提高，如图 6b、6c 所示。利用波段 5、6 计算的 NDBI 可有效突出不透水面，较好地区分较暗区域的透水面与不透水面，还可将透水区域的 ISC 去除，提高 ISC 的精度。

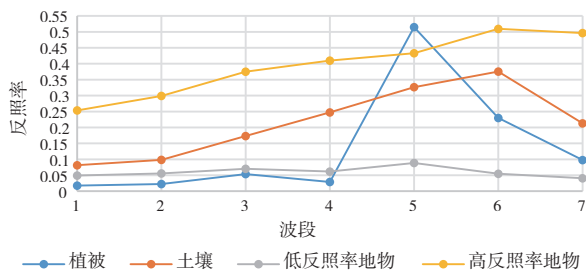


图 2 传统 PPI 端元选取的光谱特征曲线

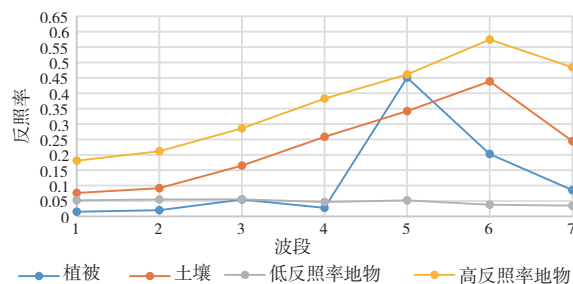


图 3 手动选取端元的光谱特征曲线

2.2 误差分析

随机选取 100 个空间分布均匀的样本区域 (图 5b), 将 3 种 LSMA 方法提取的 ISC 分别与验证数据进行比较。传统 LSMA 方法得到 ISC 的 RMS 平均值为 0.009 3, RMSE 为 0.306, R^2 为 0.898, SE 为 0.21, MAE 为 0.24; 而结合手动选取优化后的 LSMA 得到 ISC 的 RMS 平均值为 0.007 9, 从频率分布可以看出, 绝大部分像元的 RMS 值都低于 0.005, RMSE 为 0.293, R^2 为 0.932, SE

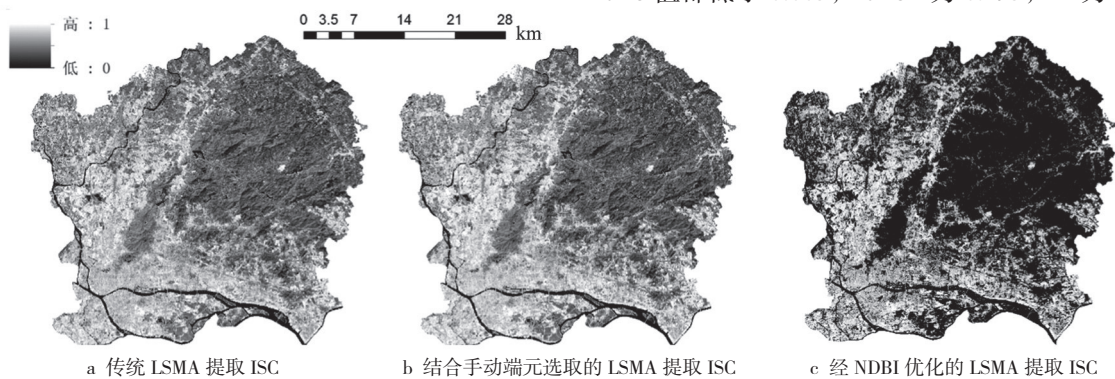


图 4 不透水面盖度结果图

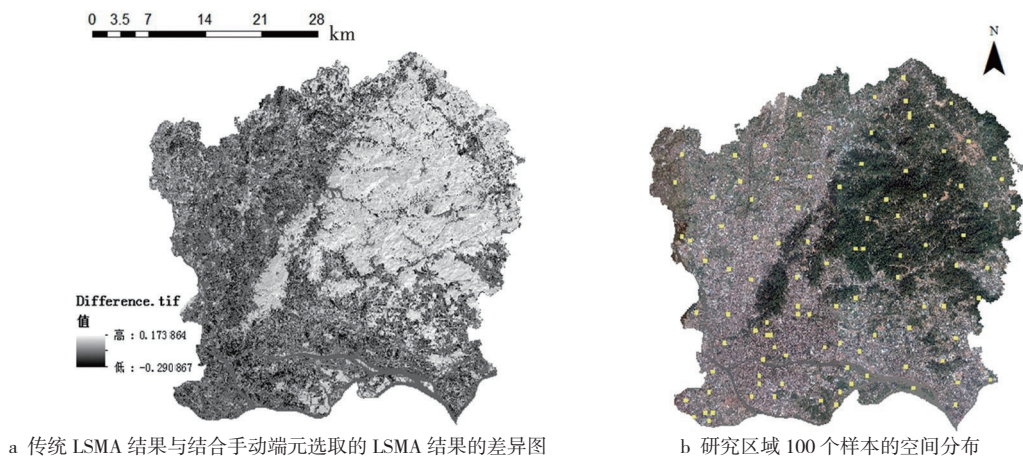


图 5 ISC 结果差异图及样本空间分布图

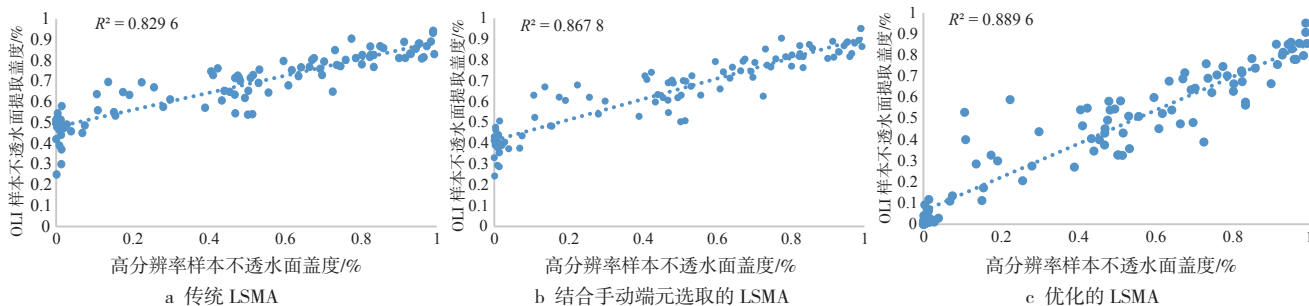


图 6 精度评价结果

为0.20, MAE为0.23。经过NDBI阈值掩膜, RMSE减少到0.125, R^2 高达0.943, SE减少为-0.035。

结合研究区实际情况, 优化线性光谱解混方法有以下作用: ①手动选取端元有利于突出不透水面与其他地物的光谱差异, 一方面可在森林等大面积区域中突出不透水面, 确保植被和不透水面的端元具有各自代表性, 扩大光谱差异, 避免混合像元问题, 另一方面使得高反照率不透水面能在大面积森林中被识别区分; ②NDBI的作用在于去除结果中大面积森林中高低反照率不透水面异常, 在像元尺度上剔除混合像元影响较大的区域, 辅助提高ISC精度。

3 结语

LSMA充分利用地物的光谱信息, 得到的组分信息具有明确的物理意义^[29]。数据表明, NDBI掩膜提高了ISC提取精度, 可检验解混过程中的重大错误; 还有效去除了透水地面的异常ISC, 可为不透水面的进一步研究提供良好基础。优化LSMA的端元选取以及NDBI阈值确定是基于大量实验获得的, 受人为因素影响, 未来可结合其他相关数据进行更为深入的探讨, 如城市夜光数据、地表温度以及研究区的GDP等, 以提高提取ISC的可信度。

参考文献

- [1] Brabec E, Schulte S, Richards P L. Impervious Surfaces and Water Quality: a Review of Current Literature and Its Implications for Watershed Planning [J]. Journal of Planning Literature Incorporating the CPL Bibliographies, 2002, 16(4): 499-514
- [2] 张燕, 王立娜, 胡毅佳, 等. 基于遥感影像的钦州市土地利用动态变化研究 [J]. 地理空间信息, 2016, 14(2): 56-59
- [3] 邹丹, 邹凯, 杨波. 基于RS与GIS的长沙市城市热岛影响因子分析 [J]. 地理空间信息, 2015, 13(1): 65-68
- [4] 陈涛, 孙安昌, 王鑫, 等. 基于遥感的武汉地区LUCC对热岛效应的影响研究 [J]. 地理空间信息, 2015, 13(1): 62-64
- [5] WENG Q H, LU D S. Landscape as a Continuum: an Examination of the Urban Landscape Structures and Dynamics of Indianapolis City, 1991~2000, by Using Satellite Images [J]. International Journal of Remote Sensing, 2009, 30(10): 2 547-2 577
- [6] Ridd M K. Exploring a V-I-S (Vegetation-impervious Surface-soil) Model for Urban Ecosystem Analysis Through Remote Sensing: Comparative Anatomy for Cities [J]. International Journal of Remote Sensing, 1995, 16(12): 2 165-2 185
- [7] WU C S, Murray A T. Estimating Impervious Surface Distribution by Spectral Mixture Analysis [J]. Remote Sensing of Environment, 2003, 84(4): 493-505
- [8] 徐涵秋, 王美雅. 地表不透水面信息遥感的主要方法分析 [J]. 遥感学报, 2016(5): 1 270-1 289
- [9] 朱艾莉, 吕成文. 城市不透水面遥感提取方法研究进展 [J].

- 安徽师范大学学报(自然科学版), 2010(5): 485-489
- [10] 刘珍环, 王仰麟, 彭建, 等. 基于不透水面指数的城市地表覆盖格局特征: 以深圳市为例 [J]. 地理学报, 2011, 66(7): 961-971
 - [11] 李瑶, 潘竟虎. 基于Landsat 8劈窗算法与混合光谱分解的城市热岛空间格局分析: 以兰州市中心城区为例 [J]. 干旱区地理, 2015, 38(1): 111-119
 - [12] 朱红雷, 李颖, 刘兆礼, 等. 基于半约束条件下不透水面的遥感提取方法 [J]. 国土资源遥感, 2014, 26(2): 48-53
 - [13] 项宏亮, 吕成文, 刘晓舟, 等. 基于SVM和线性光谱混合模型的城市不透水面丰度提取 [J]. 安徽师范大学学报(自然科学版), 2013, 36(1): 64-68
 - [14] WANG H, WU B F, LI X S. Extraction of Impervious Surface in Hai Basin Using Remote Sensing [J]. Journal of Remote Sensing, 2011, 15(2): 388-400
 - [15] 邹春城, 张友水, 黄欢欢. 福州市城市不透水面景观指数与城市热环境关系分析 [J]. 地球信息科学学报, 2014, 16(3): 490-498
 - [16] 谢慧君, 李崇巍, 张亚娟, 等. 基于光谱混合分解的流域不透水面提取及其动态分析: 以于桥水库为例 [J]. 测绘与空间地理信息, 2015, 38(10): 34-37
 - [17] 唐菲, 徐涵秋. 不同传感器线性光谱分解反演不透水面的对比: 以Landsat ETM+和EO-1 ALI为例 [J]. 武汉大学学报(信息科学版), 2013(9): 1 068-1 072
 - [18] WU C. Normalized Spectral Mixture Analysis for Monitoring Urban Composition Using ETM+ Imagery [J]. Remote Sensing of Environment, 2004, 93(4): 480-492
 - [19] 王浩, 卢善龙, 吴炳方, 等. 不透水面遥感提取及应用研究进展 [J]. 地球科学进展, 2013(3): 327-336
 - [20] 樊凤雷. 城市不透水面高光谱遥感监测研究进展 [J]. 云南地理环境研究, 2013(2): 57-64
 - [21] FAN F L, FAN W, WENG Q. Improving Urban Impervious Surface Mapping by Linear Spectral Mixture Analysis and Using Spectral Indices [J]. Canadian Journal of Remote Sensing, 2015(41): 1-10
 - [22] 徐涵秋. 一种快速提取不透水面的新型遥感指数 [J]. 武汉大学学报(信息科学版), 2008(11): 1 150-1 153
 - [23] 张熙川, 赵英时. 应用线性光谱混合模型快速评价土地退化的方法研究 [J]. 中国科学院研究生院学报, 1999, 16(2): 169-176
 - [24] WU C S, Murray A T. Estimating Impervious Surface Distribution by Spectral Mixture Analysis [J]. Remote Sensing of Environment, 2003, 84(4): 493-505
 - [25] 周存林, 徐涵秋. 福州城区不透水面的光谱混合分析与识别制图 [J]. 中国图像图形学报, 2007(5): 875-881
 - [26] 岳文泽, 吴次芳. 基于混合光谱分解的城市不透水面分布估算 [J]. 遥感学报, 2007, 11(6): 914-922
 - [27] 樊凤雷. 基于线性光谱混合模型(LSMM)的两种不同端元值选取方法应用与评价: 以广州市为例 [J]. 遥感技术与应用, 2008, 23(3): 272-277
 - [28] 查勇, 倪绍祥, 杨山. 一种利用TM图像自动提取城镇用地信息的有效方法 [J]. 遥感学报, 2003, 7(1): 37-40
 - [29] 潘竟虎, 刘春雨, 李晓雪. 基于混合光谱分解的兰州城市热岛与下垫面空间关系分析 [J]. 遥感技术与应用, 2009, 24(4): 462-468

第一作者简介: 赵怡, 博士研究生, 主要从事城市遥感提取地表径流研究。

groundwater depth, so as to evaluate the ecological effect in the mainstream of Tarim River.

Key words the mainstream of Tarim River, vegetation coverage, landscape pattern, groundwater depth (Page:77)

Design and Realization of Transportation Facility Acquisition System Based on QGIS

by LIU Jun

Abstract In order to improve the operational efficiency of transport facility acquisition, taking the high resolution remote sensing images and videos as the data source, this paper developed a transport facility acquisition system based on QGIS. The paper introduced the specific methods and steps of the system overall design, database design and function design in detail. Simultaneously, this paper analyzed the key technologies and difficulties of the system.

Key words transportation facility acquisition, QGIS, database design, linkage between video and map (Page:80)

Research on the Impact of Different Rainfall in GPS Measurement

by LING Xiaobo

Abstract We carried out GPS measurement impact analysis experiments under different rainfall conditions, and found out that a weak correlation on different rainfall and multi-path effects by pre-processing in this paper. We used GAMIT software to process many days of data through the same way. The result shows that, as the increase in rainfall, the length of baseline is increase, and this impact can reach millimeter. Therefore, in the process of high precision GPS survey or alliance calculating of IGS stations data, we must take into account the rainfall factors and rainfall situation where the IGS station, to obtain a more accurate baseline results. For general GPS measurement, because of the short observation time, it should also consider the impact of rainfall, or extend the observation time to reduce the impact.

Key words rainfall, GPS, TEQC, GAMIT (Page:84)

Panoramic Display of Electricity Information Collection Terminal Based on Open Source WebGIS

by HE Yanlan

Abstract Electricity information collection terminals have various types of faults, and it's difficult to maintain for the field staff. Combining the spatial data of collection terminal and the event data reported by collection terminal, we used open source WebGIS technology to develop a panoramic display application of electricity information collection terminal, which could provide a more convenient and efficient technology for the field staff. The operating results prove that the development of the application has reached a good balance between performance and maintenance costs, and the application lays a foundation for further expansion.

Key words WebGIS, electricity information collection terminal, open source (Page:87)

Impervious Surface Extraction Method in Guangzhou Cities Based on LSMA and NDBI

by ZHAO Yi

Abstract The data of Landsat 8 OLI in October 18, 2015 in Guangzhou were taken to extract the impervious surface with the traditional linear spectral mixture analysis (LSMA) and the modified LSMA. Based on the traditional LSMA, the manual end-member selection with pixel purity index and the normalized difference building index (NDBI) were taken to modify the LSMA. For the traditional LSMA, the RMSE was 0.306 while the correlation coefficient (R^2) was 0.898 and the systematic error (SE) was 0.21. For the modified LSMA, the RMSE was 0.125 while R^2 was 0.943, and the SE was -0.035. The accuracy assessment shows that the accuracy of the modified LSMA is significantly higher than that of the traditional LSMA and it can provide a more credible data for the further search.

Key words LSMA, manual end-member selection, NDBI, impervious surface (Page:90)

Spatial Pattern Change Monitoring and Analysis of the Traffic Network Development in Xuzhou City

by SONG Faqi

Abstract Taking Xuzhou City as the study area, this paper constructed a traffic network development spatial pattern index system from the network density and convenience, and comprehensively measured the development level of traffic network. And then, the paper used the exploratory spatial data analysis method to study the spatial pattern of the traffic network development in Xuzhou City. The results show that ①the traffic network densities of a few areas are gradually increased, and most areas (except Pizhou City) tend to balance the layout from 2015 to 2016. ②The enhancement tendency of traffic network convenience is not obvious, and the growing areas are mainly concentrated in Pizhou City. ③The traffic network convenience of the central urban area is gradually enhanced, and in most areas, the enhancements of traffic network are not obvious.

Key words traffic network, spatial pattern, geographical conditions (Page:94)

Refine Extraction of Buildings Based on the Convolutional Neural Network

by HUANG Xiaosai

Abstract The existing methods of image segmentation are often affected by image blurring and noise, so that the extracted contours are not accurate. In order to extract the accurate contours of buildings, this paper proposed an integrated approach

based on the convolutional neural network, which included building locating, shape judgment and shape matching. The experimental result shows that the proposed method can obtain accurate building contours both for DSM and multispectral images.

Key words building extraction, convolutional neural network, prior shape (Page:97)

Monitoring Analysis of the Drought in Hunan Province Based on Temperature Vegetation Drought Index

by ZHAO Jianping

Abstract In this paper, the normalized difference vegetation index (NDVI) and land surface temperature (LST) were used to construct the temperature vegetation drought index (TVDI). Combined with the topographic feature of Hunan Province, the elevation value of the TVDI fitting result was corrected, which would be better response to drought evolution rule. The processing result was divided into five levels to analysis the drought evolution. The result indicates that there are some forms of abnormal drought. The states of drought in most areas have been outstandingly alleviated until August. The standardized precipitation index (SPI) during the same time is calculated to verify that the model has certain reliability, and it can provide a good instruction to study the spatio-temporal evolution characteristics of drought.

Key words vegetation index, LST, TVDI, SPI (Page:101)

Feasibility Analysis of the RTK Height Fitting Replacing the Fourth Leveling

by CHEN Zongyong

Abstract Combined with actual production, this paper compared the RTK height fitting data with the traditional fourth leveling data, and summarized the related precise indexes. The result shows that using RTK fitting height to replace the fourth leveling is capable.

Key words GNSS, RTK, precise analysis (Page:106)

Deformation and Accident Analysis of Deep Foundation Pit Engineering

by PU Jianming

Abstract In this paper, through the comprehensive analysis of the design and construction process, field records and monitoring data of a deep foundation pit engineering, we explored the deformation rules of deep foundation pit engineering and the cause of the accident, and pointed out the shortcomings of foundation pit design and construction process.

Key words foundation pit engineering, foundation pit groundwater treatment, deformation monitoring of foundation pit, water and sand gush (Page:109)

Deformation Monitoring of the Fault Zone Based on SBAS Time-series Analysis Method

by LUO Xiang

Abstract In this paper, taking the fault zone of Haiyuan as the study area, we carried out the time-series deformation monitoring of the fault zone based on 20 scenes of Sentinel-1 data and SBAS-InSAR technology. The results show that the cumulative deformation of this study area is about -10~+5 mm. The maximum cumulative land subsidence is about 28 mm, which locates near No.1 Middle School of Haiyuan County. The fault zone of Haiyuan displays a left lateral slip, the relative rate is about 6 mm/a, which is roughly in agreement with that from GPS and geological investigations.

Key words Sentinel-1, SBAS-InSAR, the fault zone of Haiyuan, crustal deformation (Page:114)

Design and Implementation of the Livestock Products Quality Safety Monitoring System

by SUN Ruixing

Abstract Through the analysis of the specific process of Chinese livestock products safety production, this paper collected the monitoring information of livestock products quality safety form point and surface two levels, stored in the thematic database, and constructed a livestock products quality safety monitoring system. This system used GIS analysis and network to realize the query, statistic, assessment and warning analysis functions for livestock products quality monitoring data in the database, and got the position, level, type, and coverage of quality safety warning. Using GIS analysis function to carry out the early warning for the livestock products quality safety can reduce the occurrence of livestock products accident.

Key words livestock products quality safety, quality safety monitoring, GIS analysis, warning analysis (Page:117)

Research and Practice of the Stereo Map Compilation of Mountainous City

by JIANG Xue

Abstract This paper analyzed the characteristics of the commonly landform expressions from the landform stereoscopic expression. On the basis of this, according to the geographical characteristics of Chongqing City, the paper discussed the content design, technical route and key technologies of the stereo map compilation of mountainous city. This study can provide some experience for the map compilation of mountainous city.

Key words stereo map, landform expression, mountainous city, map compilation (Page:120)